Journal of Nuclear Materials 508 (2018) 168–180

Contents lists available at ScienceDirect

Journal of Nuclear Materials

journal homepage: www.elsevier.com/locate/jnucmat

Development of effective thermal conductivity model for particle-type nuclear fuels randomly distributed in a matrix

Maolong Liu [a], Youho Lee [a, *], Dasari V. Rao [b]

[a] The University of New Mexico, 1 University of New Mexico, Albuquerque, NM, 87131, USA
[b] Los Alamos National Laboratory, P.O. Box 1663, Los Alamos, NM, 87545, USA

HIGHLIGHTS

- Demonstrated a methodology for randomly distributed heat source calculation in a fuel pellet.
- Effective thermal conductivities (ETC) were calculated with and without particle heat generation.
- Demonstrated differences in ETC between with and without particle heat generation.
- Developed advanced ETC models that captures random heat source distributions.

ARTICLE INFO

Article history:
Received 15 January 2018
Received in revised form
16 May 2018
Accepted 17 May 2018
Available online 18 May 2018

ABSTRACT

Several advance nuclear reactors use particle-type Tristructural-Isotropic (TRISO) fuels randomly distributed in a matrix to allow aggressive operating conditions. Since those fuels are composites with randomly distributed TRISO particles in a matrix, suitable smearing methods are needed to obtain effective pellet-level thermomechanical properties for reactor design, and safety analysis. Currently available smearing methods for effective thermal conductivity assume uniform or no heat generation, thereby neglecting the random heat source distribution. By developing three-dimensional finite-element heat conduction models for randomly distributed heat generating kernels in a matrix, this study demonstrates that the consideration of a randomly distributed heat source is important in predicting the peak fuel temperature. In this study, (1) random packing of heat generating fuel particles introduces the statistical distribution of peak and average temperatures, and (2) those statistical temperature distributions are quantified. In light of this, thermal conductivity models with randomly distributed heat generating kernels are developed to predict peak pellet temperature for Fully Ceramic Microencapsulated (FCM) fuel and Cermet fuel for space propulsion. The developed methodology and models provide a practical methodology to predict statistically-informed peak and average fuel temperatures of nuclear fuel pellets of heat generating particles. The presented methodology is useful to quantify uncertainties in predicting nuclear fuel temperatures with TRISO particles.

1. Introduction

The Tristructural-isotropic (TRISO) fuels dispersed in a matrix are considered promising nuclear fuel candidates for several advanced reactors due to their unmatched high temperature tolerance and suitability for high burnup operations [1]. Today, several advanced reactor candidates – Fluoride-salt-cooled High-temperature Reactors (FHRs), Very High Temperature Reactor (VHTR), Fully Ceramic Microencapsulated (FCM) of Light Water Reactors (LWRs), and space propulsion reactors – are adopting TRISO fuel concepts to allow for aggressive operating conditions, economic benefits, and improved safety [2–9].

After the Fukushima accident, the recent achievements on TRISO fuel development have triggered interest to utilize TRISO fuel in LWRs or in Small Modular Reactors (SMRs) due to its superior oxidation resistance and fission product retention capabilities [10]. Oak Ridge National Laboratory (ORNL) and Ultra Safe Nuclear Corporation (USNC) proposed a TRISO-based FCM fuel concept as a potential replacement for current UO_2 fuel pellets of LWR nuclear fuel rods [8,9]. In the FCM concept, the TRISO particles are

* Corresponding author.
E-mail address: euo@unm.edu (Y. Lee).

https://doi.org/10.1016/j.jnucmat.2018.05.044
0022-3115/

embedded in a silicon carbide (SiC) matrix [11]. It is one of the accident-tolerant fuel concepts with potential enhancement on the proliferation resistance [11]. Ceramic metallic (cermet) fuel for space nuclear reactor system is another fuel type that employs randomly distributed heat generating spheres in a matrix [12]. It is generally characterized by a fuel particle of low thermal conductivity dispersed in a metallic matrix, e.g., UO_2 or uranium nitride (UN) fuel particles dispersed in tungsten [13]. It has been developed and studied since 1960's to provide significant performance and cost advantages for nuclear thermal rockets.

Despite the aforementioned advantages, the modeling challenges uniquely arising from the random distribution fuel particles introduce uncertainties in predicting neutronic, thermal, and mechanical behavior, which limit the use of the fuel concepts from the detailed reactor design and licensing standpoint [14]. In particular, prediction of fuel temperature with an effective thermal conductivity is of paramount importance for reactor design, and safety analysis. Recent efforts have focused on evaluating the effective thermal conductivity of fuel particles embedded in a matrix, in the pursuit of smearing out the pellet (or pebble) thermal behavior. The conventional approach finds effective thermal conductivity, k_e, in the pellet geometry for uniform heat generation q''', as shown in Eq. (1).

$$\nabla(k_e \nabla T) + q''' = 0 \quad \text{for } x \text{ in the entire pellet} \tag{1}$$

Eq. (1) is used for pellet-level temperature prediction by smearing spatially inhomogeneous heat generation of kernels into a uniform heat generation q'''. One widely used method to measure k_e is to apply heat flux across the geometry of interest and measure the temperature gradient across the thickness. By doing so, one can obtain k_e for the composite structures. However, the resulting temperature fields with Eq. (1) should also give a satisfactory agreement with the actual temperature fields obtained by Eqs. (2) and (3) which are coupled by equilibrium thermal boundary conditions at interfaces.

$$\nabla(k_i \nabla T) + q''' = 0 \quad \text{for } x \text{ in each heat generatin kernel i from 1 to N} \tag{2}$$

$$\nabla(k_j \nabla T) = 0 \quad \text{for } x \text{ in each non} - \text{heat generation layers j from 1 to M and matrix} \tag{3}$$

In light of this, it is reasonable to say k_e should be obtained from temperature fields with heat sources in the matrix as prescribed in Eqs. (2) and (3). Therefore, this study aims to investigate (1) temperature distribution of the pellet with random heat source distribution in matrix, (2) compare this temperature distribution with one obtained by existing correlations, (3) develop new k_e correlations based on the simulated temperature distribution with random heat source distribution, and (4) quantify the uncertainties in k_e due to random packing of heat sources.

2. Previous studies

2.1. Analytical models

Numerous models have been proposed in the literature to predict effective thermal conductivity of various types of composite materials, most of which are based on one or more of the following models: the series, parallel, Maxwell and Effective Medium Theory (EMT) [15]. For most of these models, the interfacial thermal resistance between matrix and the particles is ignored, although some studies show that it may have a relatively large influence on the effective thermal conductivity [16,17]. The Maxwell model (Eq. (4)) and the reduced Maxwell model (Eq. (5)) can also be used to calculate the effective thermal conductivity [18]:

$$\frac{k_e}{k_m} = \frac{1 + 2\beta\phi}{1 - \beta\phi} \tag{4}$$

$$\frac{k_e}{k_m} = \frac{1 - \phi}{1 + 0.5\phi} \tag{5}$$

$$\beta = \frac{\kappa - 1}{\kappa + 2} \quad and \quad \kappa = \frac{k_p}{k_m} \tag{6}$$

where k_m is the heat conductivity of the matrix, and ϕ is the packing fraction, and k_p is the equivalent heat conductivity of the fuel particle. Many modifications of the Maxwell models have been proposed to include various effects, such as the shape and size of the particle [19] as well as the interfacial thermal resistance [20]. Jeffrey [21,22] studied the heat conduction through randomly distributed spherical particles in a matrix and showed that k_e can be written as

$$\frac{k_e}{k_m} = 1 + K_1\phi + K_2\phi^2 + \cdots + K_n\phi^n + \cdots \tag{7}$$

where the coefficient K_n shows the effect on the conductivity of n-particle interactions. The Maxwell model and the reduced Maxwell model is a simplified model of Eq. (7) by ignoring thermal interactions between particles, and by only taking into account the first-order term [23,24]. Hence, the Maxwell model is only valid for packing fraction up to about 25% [17,25,26]. Chiew and Glandt [23] improved the Maxwell model by considering the higher order interaction between particles and derived the following effective thermal conductivity correlation:

$$\frac{k_e}{k_m} = \frac{1 + 2\beta\phi + \left(2\beta^3 - 0.1\beta\right)\phi^2 + 0.05\phi^3 e^{4.5\beta}}{1 - \beta\phi} \tag{8}$$

Gonzo [24] compared experimental results of different porous materials with Eq. (8) estimations and it shows a good agreement.

Another commonly-used model for effective thermal conductivity estimation is an EMT developed by Bruggeman [17,27], which does not distinguish the matrix and the particles, and treats local conductivities as fluctuations about the conductivity of a uniform medium [25]. The Bruggeman model is shown in Eqs. (9) and (10).

$$\frac{k_e}{k_m} = \kappa A + \sqrt{\kappa^2 A^2 + 0.5\kappa} \tag{9}$$

$$A = 0.25\left(3\phi - 1 + \frac{2 - 3\phi}{\kappa}\right) \tag{10}$$

The Bruggeman model was compared with measured thermal

conductivities of cermet fuel with 60% and 80% packing fraction. It shows a good agreement with the 80% packing fraction but less satisfactory agreement with the 60% packing fraction case [28].

In summary, the existing thermal conductivity models for composite structure are developed to give effective thermal conductivity as a function of packing fraction and individual kernel and matrix properties. However, all of them assume no heat generation in individual kernels. This implies that the existing models can be readily used for typical particle-reinforced composites that do not generate heat. However, its validity for the temperature prediction of nuclear fuel pellets with heat generating kernels randomly embedded in a matrix is not understood.

2.2. Numerical simulation

Numerical simulation is one way to estimate the effective thermal conductivity for composite materials [15,17,29]. Nozad et al. [30] developed a closure model for spatially periodic porous media. Cruz and Patera [31] proposed a scale-decoupling procedure to solve the effective property using a periodic boundary. This method was later used by several researchers to calculate the effective thermal conductivity for composite materials [32]. The use of these repetitive structures ignored the fact the randomness of the particles inside the matrix can significantly affect the accuracy of the results [14]. Folsom et al. [25] developed a model to calculate the effective thermal conductivity of a FCM fuel pellet with homogenous particles distributed randomly in the matrix. They concluded that Chiew and Glandt model [23] is the most accurate model for packing fraction from 0.18 to 0.40. However, they did not report the impact of randomness of the TRISO particles on the FCM fuel pellet effective thermal conductivity. Hence, the study suggests the necessity of having additional geometric information about the media other than the packing fraction for improved estimation of the effective properties [33]. Oppelt et al. [34] and Cho et al. [35] simulated the effective thermal conductivity of material system consisting of a continuous phase and discrete particles, and concluded that the effective thermal conductivity is influenced significantly by particle shape, distribution and orientation.

3. Method: numerical simulation

In this study, three-dimensional finite-element method (FEM) heat conduction models were used to investigate temperature distribution of reference fuel pellets with randomly distributed heat sources in a matrix. The calculated temperature distributions were compared with those obtained by existing k_e models that do not take into account the heat generation in kernels. The obtained temperature fields are used to support new effective thermal conductivity correlation developments and quantify uncertainties in effective thermal conductivity due to random packing of heat sources.

3.1. Reference fuel designs

This section presents information of reference pellet designs – FCM and Cermet fuel pellets – used for simulation.

3.1.1. FCM fuel pellet

A full size FCM fuel pellet is simulated in this study. As illustrated in Fig. 1, each randomly dispersed TRISO fuel particle consists of a spherical kernel of uranium nitride (UN) surrounded by four coating layers. The innermost coating layer is a porous carbon buffer layer, and is followed in turn by an inner pyrolytic carbon (IPyC) layer, a silicon carbide (SiC) layer, and an outer pyrolytic carbon (OPyC) layer [3]. Table 1 provides the dimensions, and

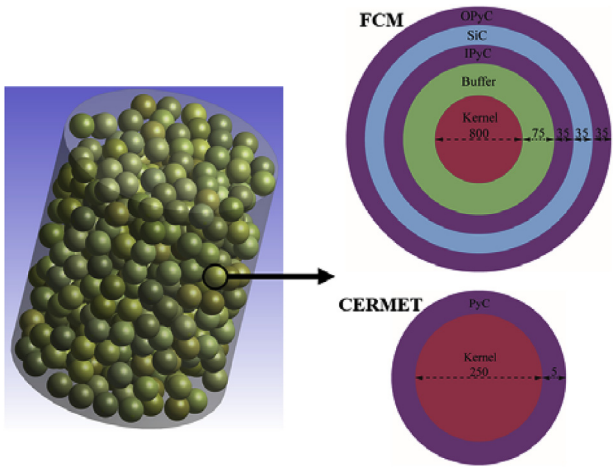

Fig. 1. Simulated cermet fuel pellet with randomly distributed fuel particles (dimensions in μm).

thermal conductivity of the reference fuel particle and the matrix used in the simulation. The design parameters of the FCM fuel pellet are summarized in Table 2. The thermophysical properties of the TRISO fuel particle and the matrix were determined from multiple sources [6,9,11,36]. The range of packing fractions shown in Table 2 were tested investigate packing fraction-sensitive uncertainties in the effective thermal conductivity calculation.

3.1.2. Cermet fuel pellet

The simulated cermet fuel pellet is shown in Fig. 1. The UN fuel kernel is surrounded by a PyC layer. The fuel particles are embedded in a tungsten matrix. Physical properties of the reference particle and matrix are shown in Table 3. As shown in Table 4, three different pellets sizes were simulated. For all three cases, both the packing fraction and the aspect ratio of the pellet were kept constant.

3.2. Numerical approach

Steady-state heat conduction simulations of a FCM fuel pellet and a cermet fuel pellet were conducted using ANSYS 18.0. All constituent layers of the fuel particles were explicitly modeled in this study. For the random particle generation, a separate computer code that generates random packing of particle fuels in a matrix for a target packing fraction was developed based on the following steps: (1) The initial locations of all particles were generated randomly within the domain. (2) If two or more particles overlap, these overlapped particles were moved randomly to new locations in the domain. (3) Step (2) was repeated until no particles overlap with each other. This code was linked to the ANSYS 18.0 for geometry import, property assignments, and mesh generation. For all of the presented cases, mesh sensitivity studies were performed to verify mesh independence. Fig. 2 shows the mesh of the FCM pellet and the TRISO fuel particles used for this study. All layers of the TRISO fuel particles were modeled in this study.

4. Verification of simulation: effective thermal conductivity without heat generation

As a first step to verify the sanity of the thermal conductivity simulation, effective thermal conductivities for composites without heat generation were obtained. By doing so, the agreement between the calculation results and existing models were compared, all of which do not account for heat generation. Besides verifying

Table 1
Reference parameters of the UN TRISO particle used in this study [6,9,11,36].

Layer	Outer radius (μm)	Thermal conductivity [W/(m·K)]
UN kernel	400.0	22.5
Buffer	475.0	0.5
IPyC	510.0	4.0
SiC	545.0	10.0
OPyC	580.0	4.0
Matrix (irradiated NITE SiC)	–	10.0

Table 2
Details of the FCM fuel pellet design parameters [9].

FCM pellet configuration	Value
Packing fraction	0.25–0.50
Number of TRISO particles	278–556
FCM pellet diameter	9.9 mm
FCM pellet length	11.8 mm
Linear heat rate of the pellet	201.70 W/cm

Table 3
Reference parameters of the cermet fuel pellet used in this study [6,37].

Layer	Outer radius (μm)	Thermal conductivity [W/(m·K)]
UN kernel	125.0	32.90
PyC	130.0	4.0
Matrix (Tungsten)	–	95.20

Table 4
Details of the cermet fuel pellet configuration.

Cermet pellet configuration	Value
Kernel	UN
Particle diameter	0.26 mm
Packing fraction	0.55
UN kernel power density	1700.0 MW/m^3

the presented simulation framework, this work supports the computational validation of the existing analytical models. The effective thermal conductivity of FCM and Cermet fuel pellet with a packing fraction varying from 0.25 to 0.55 were calculated by following the procedure described in previous studies [25] and [38]. The following boundary conditions were applied to evaluate the effective thermal conductivities without heat generation in the fuel particles.

4.1. Boundary conditions

For both FCM and Cermet fuel pellet, a constant temperature (300.0 °C) was applied to one side and a constant heat flux (0.1 MW/m^2) was applied to the other side of the pellet, as shown in Fig. 3. The adiabatic boundary condition was applied on the side of the pellet. Following the Fourier's Law [25], the effective thermal conductivity of the pellet was obtained using the average of the temperature at both ends of the pellet (one imposed as the boundary condition and the other calculated) and the imposed heat flux at the top surface of the pellet.

4.2. Effective thermal conductivity simulation results

First, 60 calculations of the FCM pellet with packing fraction $\phi = 0.3$ were carried out to investigate the impact of particle

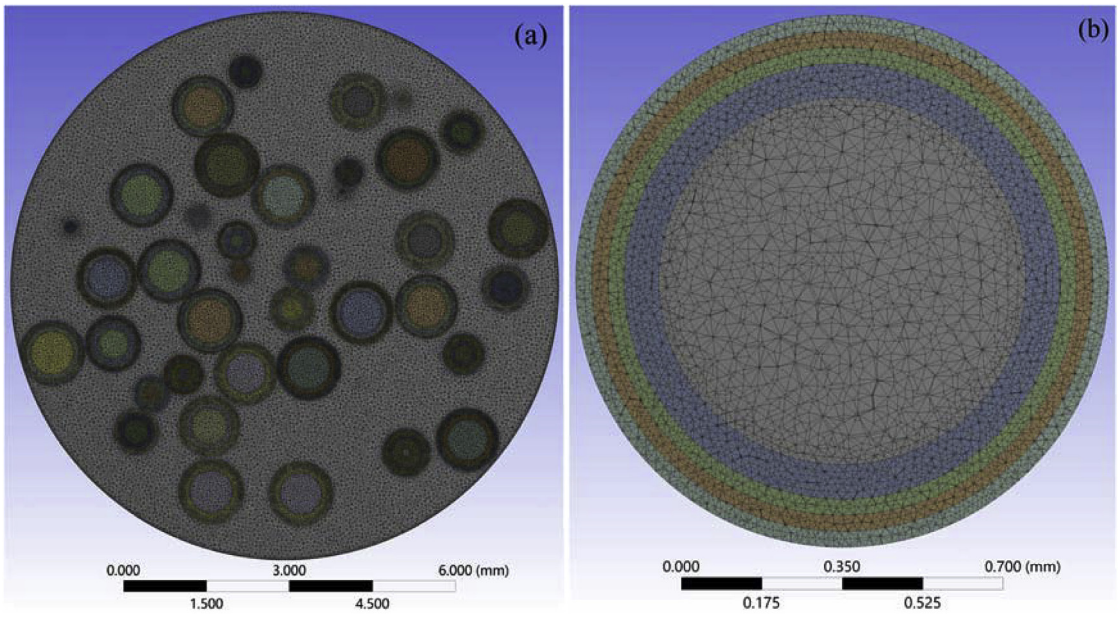

Fig. 2. Finite element mesh for the FCM pellet with total of 20,607,942 triangle elements and 37,590,244 nodes: (a) cross-section of the FCM pellet, and (b) cross-section of a TRISO fuel particle.

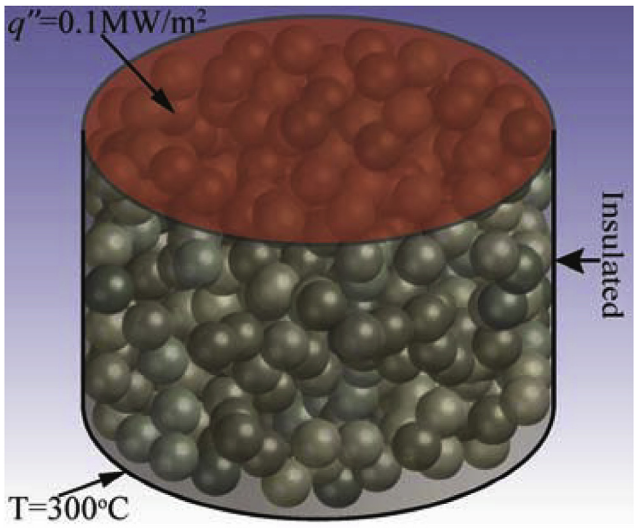

Fig. 3. Simulation domain and the boundary conditions to calculate the effective thermal conductivity.

randomness on the effective thermal conductivity. As shown in Fig. 4, the calculated effective thermal conductivity value follows a normal distribution with mean value $\mu = 7.797$ W/(m·K) and standard deviation $\sigma = 0.007$ W/(m·K). As range of the possible effective thermal conductivity caused by the TRISO particle distribution is less than 0.6% of the average effective thermal conductivity, the influence of random distribution can be ignored for fuel pellet without heat generation. These results prove that the mean effective thermal conductivity of the pellet is insensitive to the geometry arrangement of a large number of particles with true random distribution [38]. Hence, as shown in Fig. 5 and Table 5, a single calculation with randomly distribution particles was conducted to obtain the effective thermal conductivity for each packing fraction.

The obtained effective thermal conductivities of simulated results are compared with the analytically obtained effective thermal conductivities. Fig. 5 and Table 5 summarize the comparisons. In order to apply the two-phase analytical models presented in section 2.1, the effective thermal conductivity of the TRISO particle was first calculated with an analytical model indicated in Ref. [38]. The calculated effective thermal conductivity of the TRISO fuel particle, k_{TRISO}, for FCM fuel and cermet fuel is 3.77 W/(m·K) and 24.27 W/(m·K), respectively. The Maxwell model and the reduced Maxwell model ignored thermal interactions between particles, and only took into account the first-order term. Chiew and Glandt [23] improved the Maxwell model by considering the higher order interaction between particles. Thus, as shown in Fig. 5, the Chiew and Glandt [23] model gives the best agreement with the simulated results in the entire range of tested packing fractions (0.25–0.55). Folsom et al. [25] also suggested the same conclusion in their study.

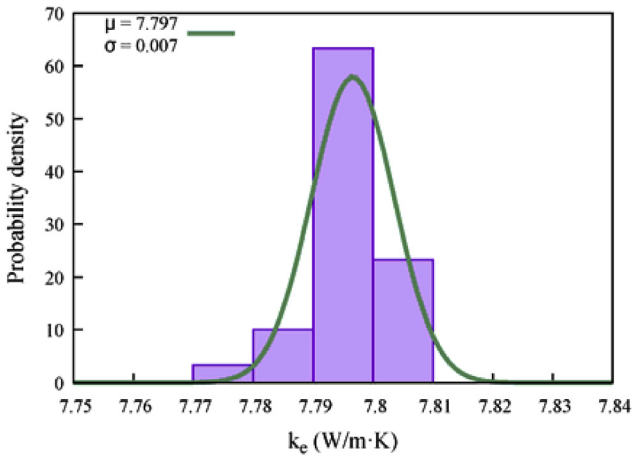

Fig. 4. Distribution of the calculated effective thermal conductivity of the FCM fuel pellet with packing fraction $\phi = 0.3$.

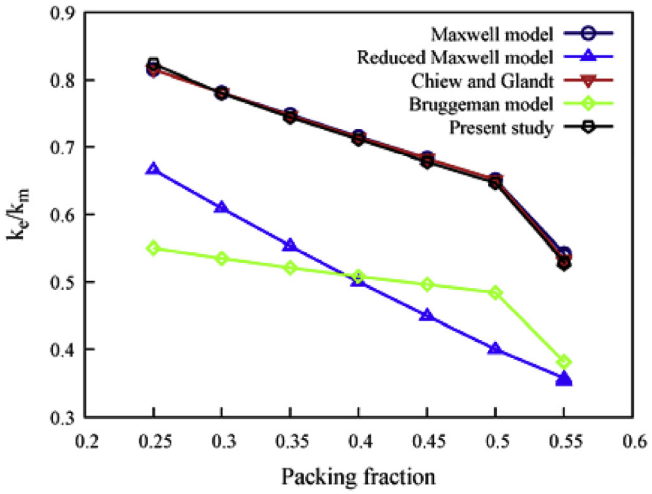

Fig. 5. Calculated effective thermal conductivity vs analytical models.

5. Simulation of effective thermal conductivity with heat generation

To evaluate the effect of heat generation in the fuel particles, effective thermal conductivities for composites with heat generation were obtained with simulation. Full-scale FCM fuel pellets with a packing fraction varying from 0.35 to 0.45 and three different cermet fuel pellets with the same packing fraction were simulated. Uniform heat generation was assumed in individual fuel kernels. For each case, 60 calculations were performed to investigate the influence of the particle randomness.

5.1. Boundary conditions

As shown in Fig. 6 (a)-(b), a fixed temperature boundary condition was applied to the lateral surface of both pellets - 442.0 °C for the FCM pellet [6] and 2026.85 °C for the cermet pellet. The adiabatic boundary condition was applied on both ends of the pellet.

A linear power of 201.7 W/cm was applied to the FCM pellet [9]. The volumetric power of an individual fuel kernel, which varies with the packing fraction, was determined by the following equation:

$$q_1''' = \frac{q'_{pellet} L}{N V_1} \tag{11}$$

where q'_{pellet} is the linear power of the pellet, L is the height of the pellet, N is the total number of particles in the pellet which depends on the packing fraction, and V_1 is the volume of the fuel kernel. The number of fuel particles and their volumetric power for each simulated packing fraction are summarized in Table 6. The kernel volumetric heat generation is larger for smaller packing fraction.

For the simulation of cermet fuel, a fixed volumetric power for

Table 5
Comparison of the numerical simulation results at various particle-volume fractions to the analytical effective thermal conductivity models.

Pellet	Packing fraction	Calculated k_e W/(m·K)	Maxwell model		Reduced Maxwell model		Chiew and Glandt model		Bruggeman model	
			k_e	%Diff	k_e	%Diff	k_e	%Diff	k_e	%Diff
FCM	0.25	8.23	8.15	−0.97	6.67	−18.95	8.15	−0.97	5.50	−33.17
	0.30	7.80	7.81	0.13	6.09	21.92	7.81	0.13	5.35	−31.41
	0.35	7.44	7.48	0.54	5.53	−25.67	7.47	0.40	5.21	−29.97
	0.40	7.11	7.15	0.56	5.00	−29.68	7.14	0.42	5.08	−28.55
	0.45	6.78	6.83	0.74	4.49	−33.77	6.83	0.74	4.96	−26.84
	0.50	6.47	6.52	0.77	4.00	−38.18	6.52	0.77	4.84	−25.19
Cermet	0.55	50.39	51.61	2.42	34.02	−32.49	50.82	0.85	36.36	−27.84
	0.55	50.16	51.33	1.45	33.66	−32.89	50.53	0.74	36.28	−27.67
	0.55	50.25	51.28	2.05	33.59	−33.15	50.48	0.46	36.27	−27.82

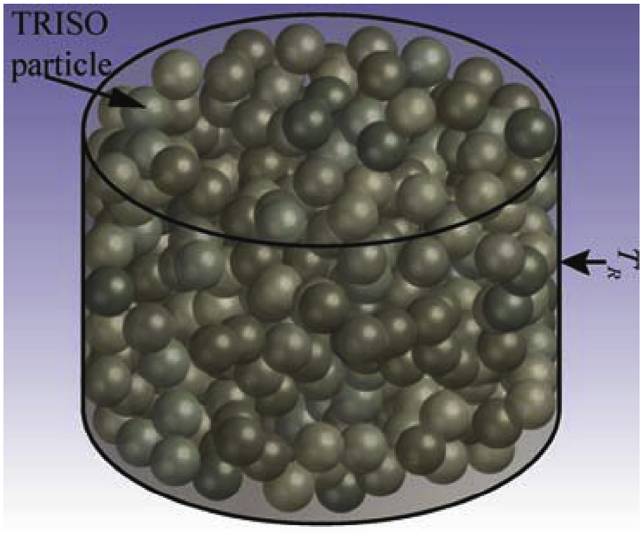

Fig. 6. Fuel pellet and simulation model: $T_R = 442.0\,^{\circ}C$ for the FCM pellet, and $T_R = 2026.85\,^{\circ}C$ for the cermet pellet.

individual kernels was used while the size of the pellet increases with the same aspect ratio (Table 7). By doing so, the effect of pellet size on the statistical nature of random packing on pellet temperature was investigated.

Before leaving this section, it is important to point out the constraints of this simulation due to assumptions and boundary conditions presented in this section. The simulation of FCM/CERMET fuel pellet consisting of randomly distributed heat-generating particles was carried out based on the following assumptions: (1) uniform heat generation was assumed in individual fuel kernels by ignoring the power distribution along the axial/radial direction of the pellet; (2) the temperature dependence of the thermal conductivity of the fuel particle and the matrix was assumed constant; and (3) adiabatic boundary conditions were used on both end of the fuel pellet by ignoring the axial heat transfer between pellets caused by non-uniform power distribution along the axial direction of the reactor core. These assumptions simplified this study such that the simulation results were only influence by the particle randomness.

5.2. Simulation results and discussion

Contour plots for the temperature distribution of a FCM pellet and kernels are shown in Fig. 7 (a) and (b). The temperature distribution from both figures shows there exists a cylindrical "hot zone" at the center of the pellet where the fuel kernels have the highest temperature. This is in agreement with the analytical temperature representation of fuel pellet with uniform heat generation. Yet, the simulated results with the heat generation in individual kernels shows that the calculated temperature distribution, hence the peak temperature, exhibits departure from the uniform heat generation temperature curve because of the random packing of heat generating kernels, as shown in Fig. 7 (c).

For each simulation case presented in Tables 6 and 7, 60 random packing arrangements were simulated to investigate the statistical nature of temperature distribution with randomly distributed heat sources. Fig. 8 shows peak kernel temperature of 60 simulation cases and fitted statistical distribution. As anticipated, the randomly distributed heat sources lead to the statistical

Table 6
Fuel particle number and volumetric power of FCM fuel pellet for the reference pellet linear heat generation $q'_{pellet} = 201.7$ W/cm.

Packing fraction	Number of fuel particles in a pellet	Fuel particle volumetric power (MW/m^3)
0.35	389	2282.8
0.40	444	2000.0
0.45	500	1776.0

Table 7
Particle number and power density of fuel kernel for cermet fuel pellet.

Packing fraction	Pellet size		Particle number	Fuel kernel power density (MW/m^3)
	Diameter (mm)	Height (mm)		
0.55	2.25	1.50	356	17000.00
0.55	2.40	1.60	432	17000.00
0.55	2.70	1.80	616	17000.00
0.55	3.00	2.00	845	17000.00

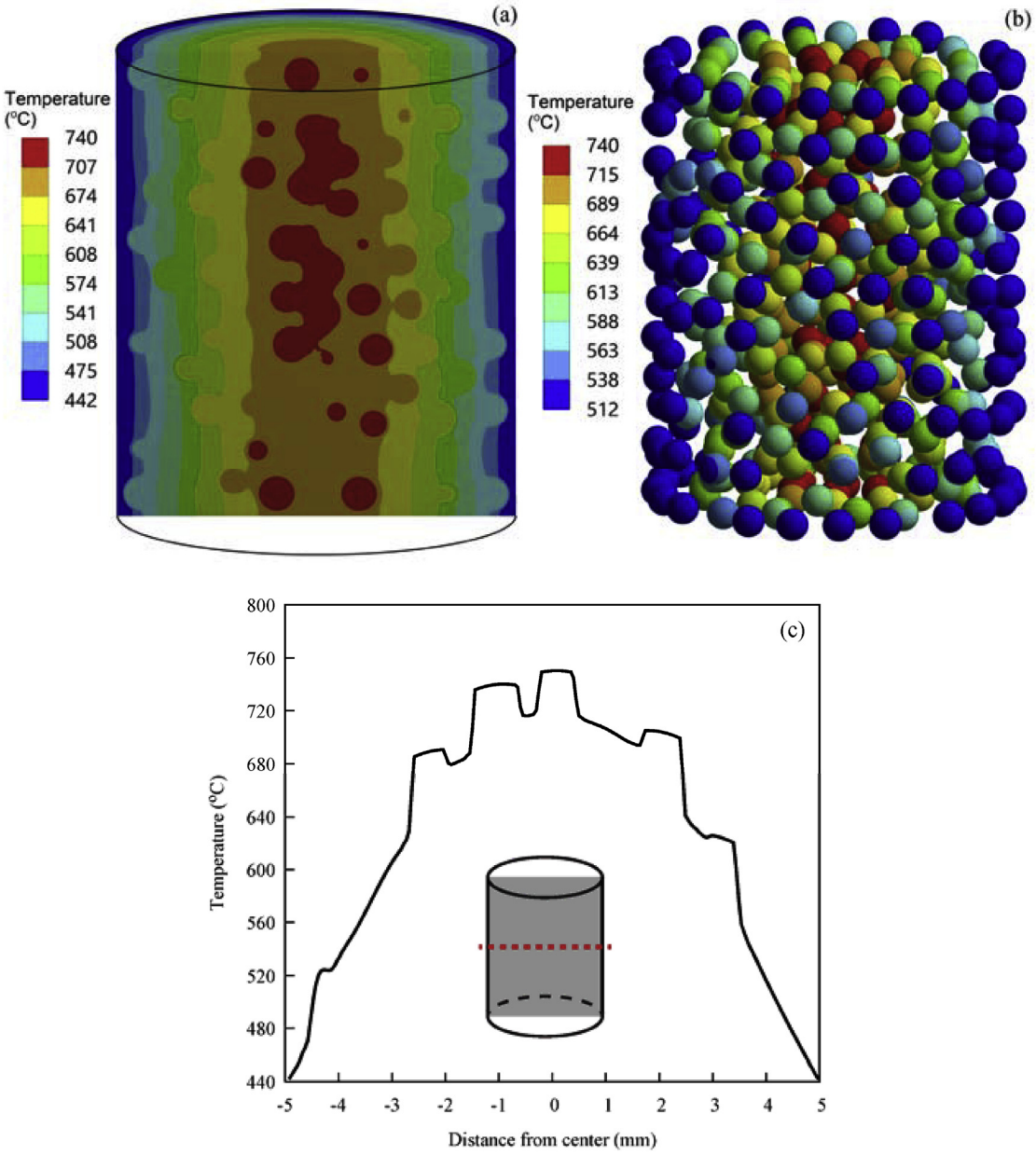

Fig. 7. Temperature contour of the FCM fuel pellet and the fuel kernels (packing fraction $\phi = 0.45$): (a) fuel pellet; (b) fuel kernels; (c) Radial temperature distribution at the center of the pellet.

distribution of the maximum temperature for the same pellet design. As shown in Fig. 9, the statistical distributions in peak particle temperature, pellet centerline average temperature, and pellet average temperature follow the normal distribution whose mean μ and standard deviation σ can be identified. It is worth noting that the standard deviation of the temperature distributions shown in Fig. 9 (a)-(c) decreases with a higher packing fraction. This is because the degree of freedom in the particle arrangement reduces with a higher packing fraction, thereby leading to a more deterministic arrangement of fuel particles. The fuel particle effective thermal conductivities, k_{TRISO}, for FCM (3.77 W/m·K) is lower than that of the matrix thermal conductivity (10.0 W/m·K). Hence, the pellet with a lower packing fraction should give a higher effective thermal conductivity without consideration of heat generation. However, on the other hand, the volumetric heat generation of individual fuel kernel increases with a lower packing fraction for a fixed pellet power. In these competing phenomena, it was found that the later outweighs the former as the peak pellet temperature increases with the lower packing fraction for the reference FCM fuel pellet. Hence, for the reference FCM and cermet fuel design, peak particle temperature and pellet centerline average temperatures increase with lower packing fraction. But the pellet average temperatures decrease with lower packing fraction as the overall thermal conductivity of the pellet decrease with higher packing fraction.

Fig. 10 shows peak particle temperature, pellet centerline average temperature, and pellet average temperature of the reference cermet fuel. The peak particle temperature as well as the average temperatures increases with the increasing pellet size as the thermal resistance increases. It noteworthy that the standard deviation increases with the pellet size. This is because a larger pellet volume allows a higher degree of freedom for random

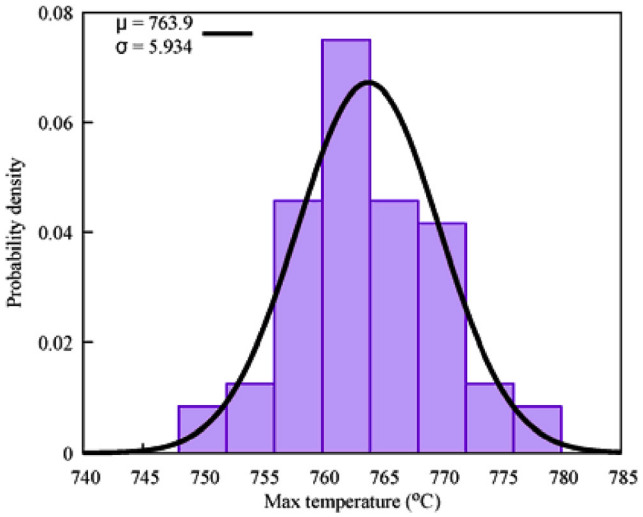

Fig. 8. Maximum particle temperature distribution of the reference FCM pellet with packing fractions $\phi = 0.35$.

particle arrangement, thereby giving a larger variation in the particle arrangements.

The presented statistical distributions for temperature can be used to obtain the corresponding statistical distribution of effective thermal conductivity. The following section discusses the calculation for effective thermal conductivities with the obtained temperature distributions.

5.3. Effective thermal conductivity estimation based on the homogeneous model

The obtained pellet temperature illustrated in Fig. 7 shows that the peak pellet temperature with the random heat source distribution is not necessarily positioned at the center ($r = 0$) for randomly distributed heat sources. The effective thermal conductivities in this study are found as a thermal conductivity value that gives the same target temperature using uniform heat generation. Hence, thermal conductivities based on peak particle temperature (k_{peak}), fuel pellet centerline average temperature (k_{axis}), and fuel pellet average temperature (k_{avg}) can be calculated using the following equations obtained by the 1-D radial heat diffusion equation in cylindrical coordinates with a uniform heat generation,

$$k_{peak} = \frac{q'''_p R_p^2}{4(T_{p,\max} - T_R)} \tag{12}$$

$$k_{axis} = \frac{q'''_p R_p^2}{4(T_{axis,avg} - T_R)} \tag{13}$$

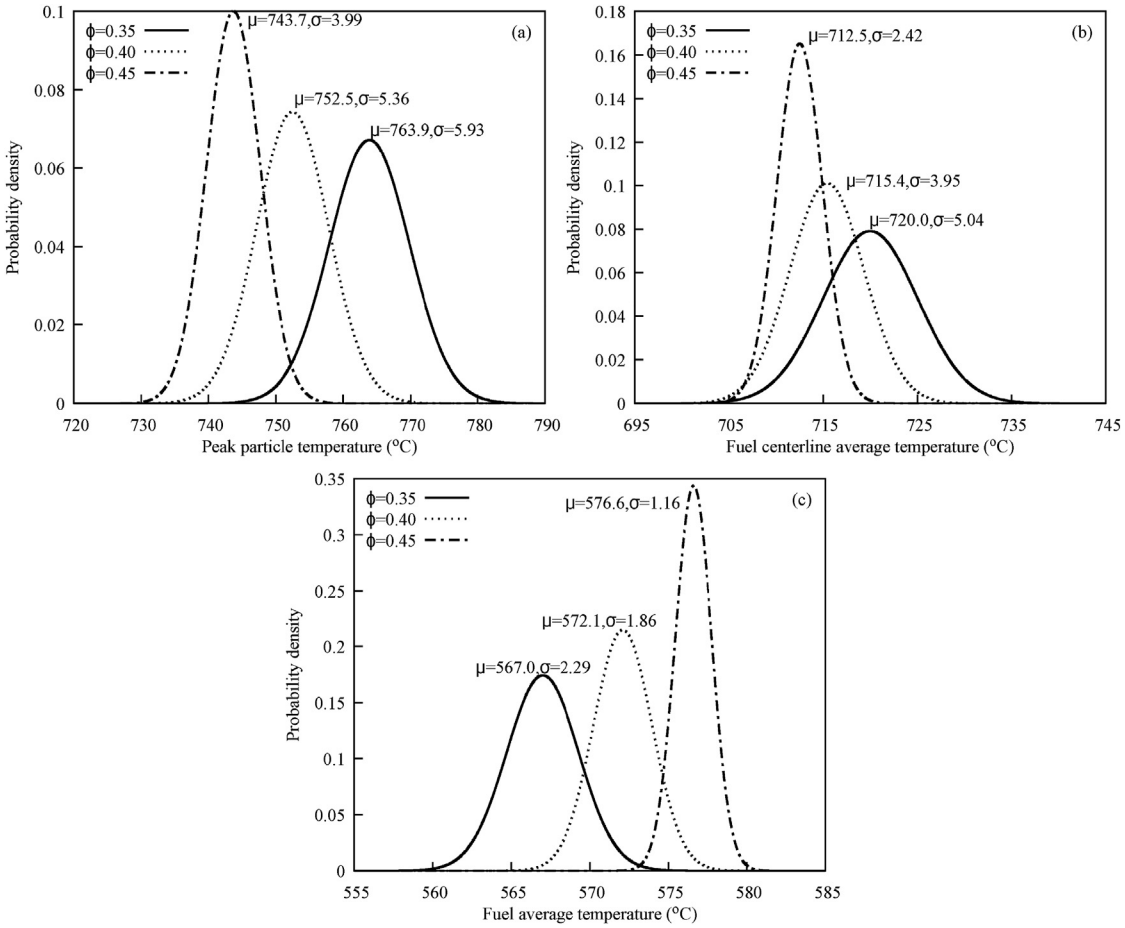

Fig. 9. Temperature distribution of the reference FCM pellet for different packing fractions (ϕ): (a) peak particle temperature; (b) pellet centerline average temperature; (c) pellet average temperature.

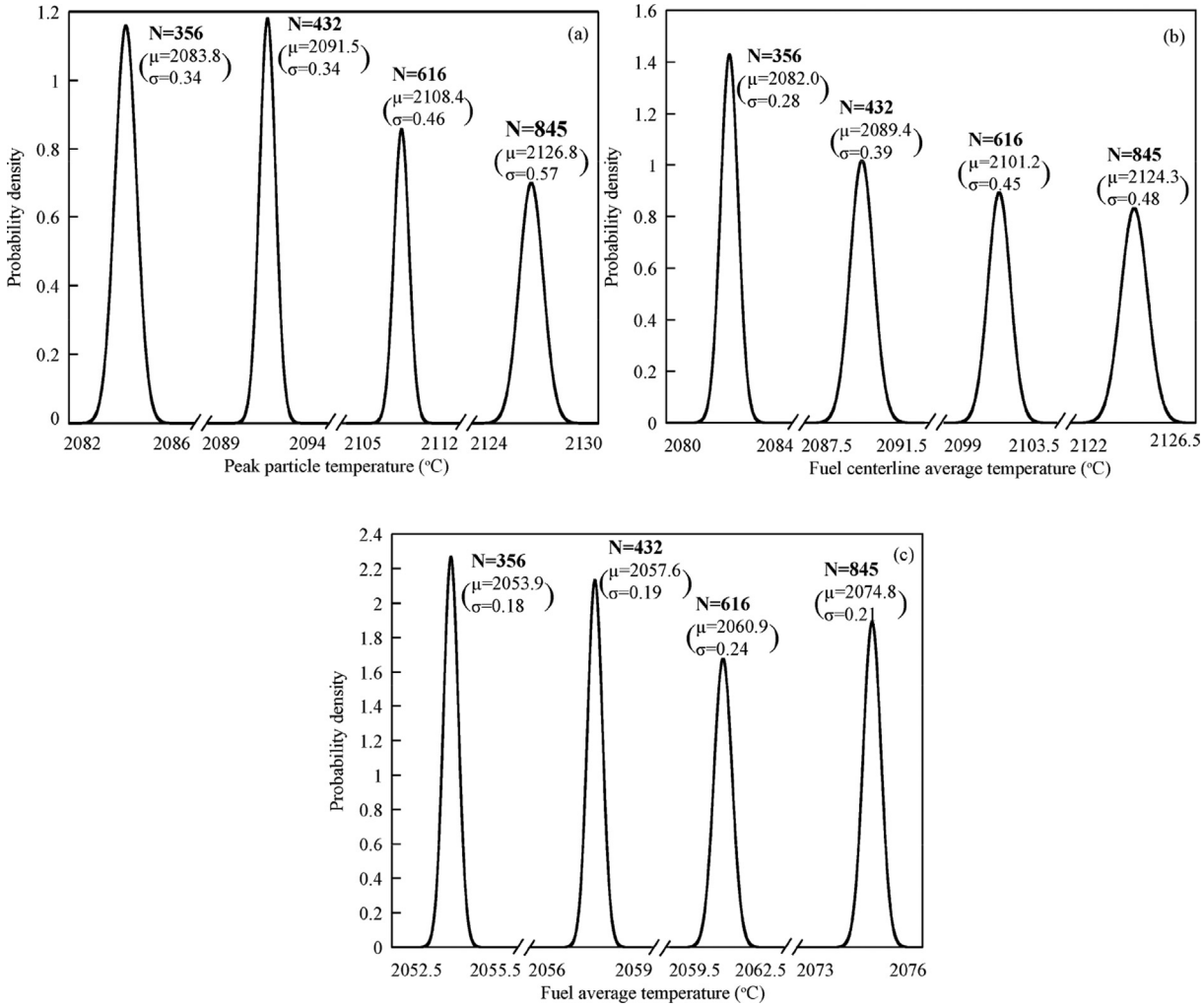

Fig. 10. Temperature distribution of the reference cermet pellet for different pellet sizes with the fixed kernel volumetric heat generation and packing fraction ($\phi = 0.55$): (a) peak particle temperature; (b) pellet centerline average temperature; (c) pellet average temperature.

$$k_{avg} = \frac{q'''_p R_p^2}{8(T_{avg} - T_R)} \quad \text{with} \quad T_{avg} = \frac{\iiint T dV}{V_{pellet}} \tag{14}$$

where $T_{p,max}$ is the peak temperature of the fuel particle simulated with randomly distributed heat sources, T_R is the surface temperature of the pellet, R_p is the radius of the pellet, $q'''_p = \frac{NV_1 q'''_1}{V_{pellet}}$ is the pellet's volumetric heat generation rate, $T_{axis,avg}$ is the pellet centerline average temperature, and T_{avg} is the average temperature of the fuel pellet. By doing so, one can obtain the target temperature of a pellet (either peak temperature or average temperatures) with random heat source distribution by solving the heat diffusion equation of uniform heat generation with the obtained effective thermal conductivity.

Fig. 11 (a)-(c) show the obtained effective thermal conductivity distributions of the reference FCM pellets based on the peak particle temperature, fuel pellet centerline average temperature, and fuel pellet average temperature distributions of randomly distributed heat sources, and effective thermal conductivity values calculated by the conventional composite models that do not take into account non-uniform heat generation. As the effective thermal conductivities are inversely proportional to the corresponding fuel pellet temperature (see eq. 12–14), the obtained effective thermal conductivities follow a normal distribution as well. It is noticeable that the differences between the effective thermal conductivities evaluated with and without non-uniform heat generation due to randomly distributed heat sources are significant in general. The Bruggeman model and reduced Maxwell model give the best agreement with k_{peak} among the other models while k_{avg} shows better agreement with Chiew and Glandt model with the increasing of packing fraction. It is also worth to point out that the disagreements between k_{peak}, k_{axis} and k_{avg} get smaller with higher packing fraction.

Fig. 11 (d) and (e) summarizes the mean effective thermal conductivity and standard deviation of the normal distribution for all three packing fractions simulated. The mean and standard deviation of the effective thermal conductivities are proportional to the packing fraction. While the effective thermal conductivities follow the normal distribution, their mean (μ) and standard deviation (σ) can be expressed as a linear function of packing fraction (ϕ), as shown in Eq. 15–20.

$$\mu\left(\frac{k_{peak}}{k_m}\right) = 0.335\phi + 0.382 \qquad (0.35 \le \phi \le 0.45) \tag{15}$$

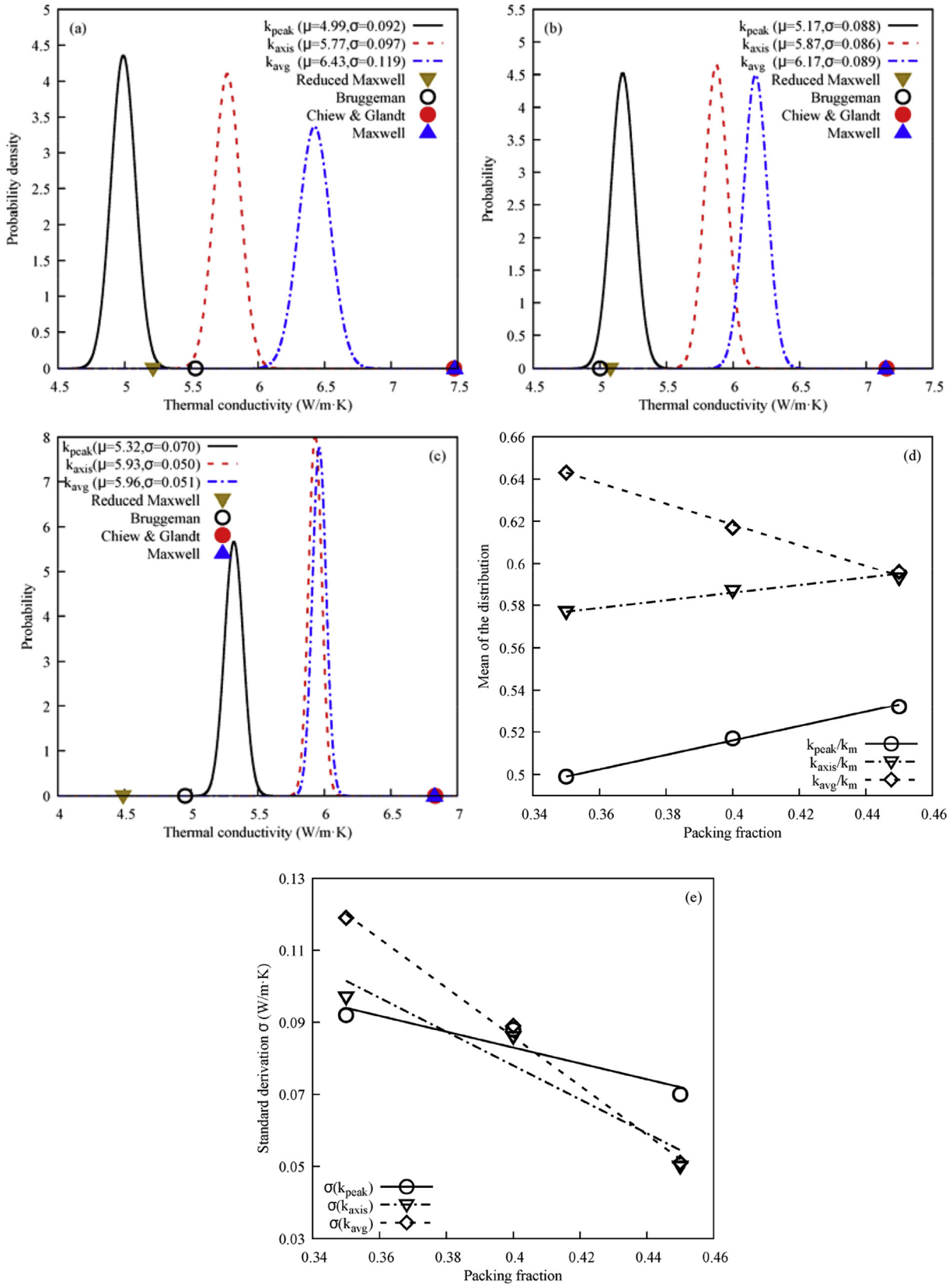

Fig. 11. Distribution of the thermal conductivities of the FCM fuel pellet for different packing fractions: (a) $\phi = 0.35$; (b) $\phi = 0.40$; (c) $\phi = 0.45$; mean value μ (d) and standard deviation σ (e) of the effective thermal conductivities following the normal distribution.

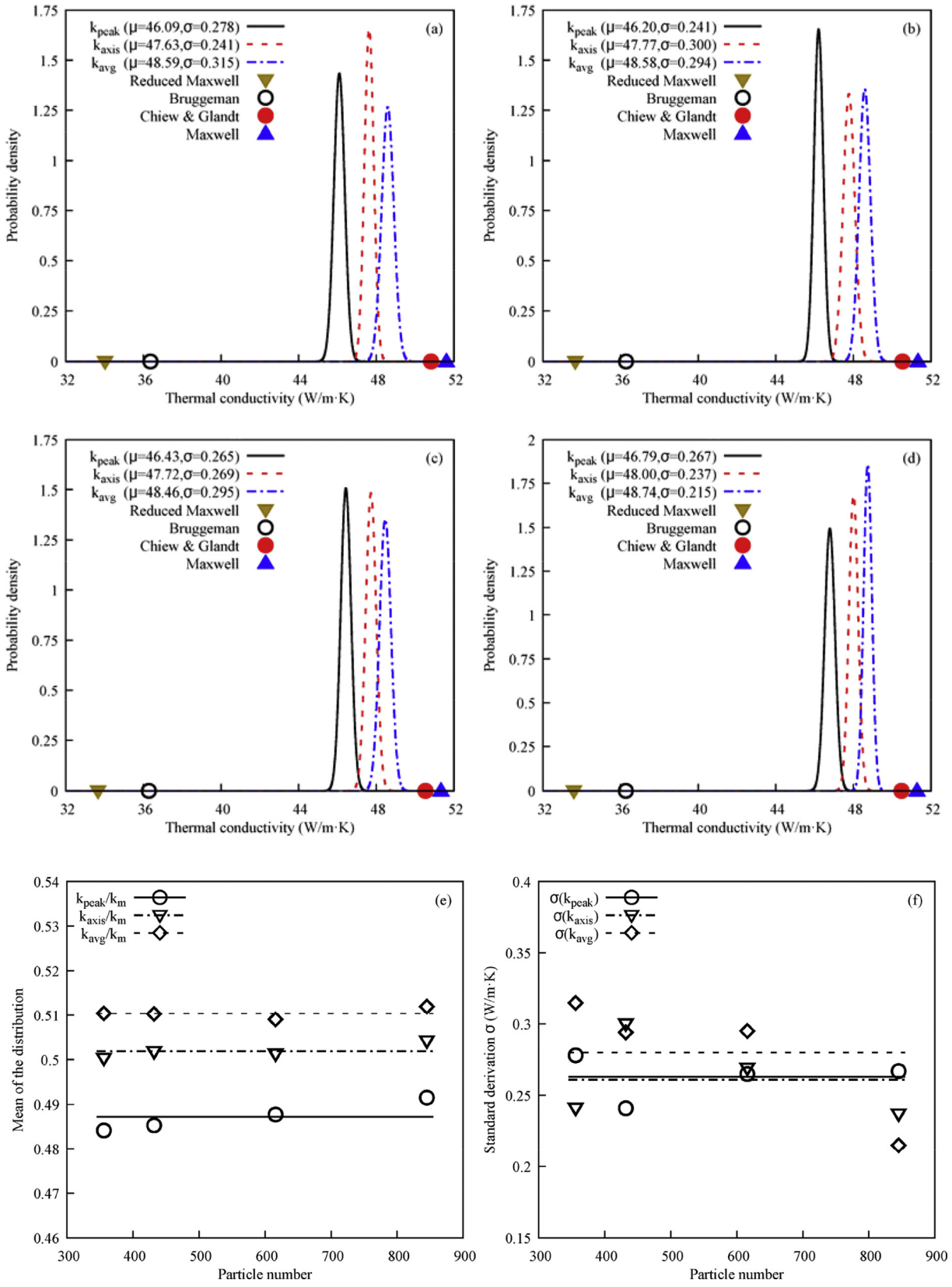

Fig. 12. Distribution of the calculated effective thermal conductivity of the cermet fuel pellet ($\phi = 0.55$): (a) Number of particles, N = 356; (b) N = 432; (c) N = 616; (d) N = 845; mean value μ (e) and standard deviation σ (f) of the calculated effective thermal conductivities.

$$\sigma\left(\frac{k_{peak}}{k_m}\right) = -0.220 + 0.171\phi \qquad (0.35 \le \phi \le 0.45) \tag{16}$$

$$\mu\left(\frac{k_{axis}}{k_m}\right) = 0.160\phi + 0.522 \qquad (0.35 \le \phi \le 0.45) \tag{17}$$

$$\sigma\left(\frac{k_{axis}}{k_m}\right) = -0.470 + 0.266\phi \qquad (0.35 \le \phi \le 0.45) \tag{18}$$

$$\mu\left(\frac{k_{avg}}{k_m}\right) = -0.470\phi + 0.807 \qquad (0.35 \le \phi \le 0.45) \tag{19}$$

$$\sigma\left(\frac{k_{avg}}{k_m}\right) = -0.680 + 0.358\phi \qquad (0.35 \le \phi \le 0.45) \tag{20}$$

Fig. 12 (a)-(d) show the obtained effective thermal conductivity distributions of the reference cermet fuel pellet based on the peak particle temperature, fuel pellet centerline average temperature, and fuel pellet average temperature distributions of randomly distributed heat sources, and effective thermal conductivity values calculated by the conventional composite models that do not take into account non-uniform heat generation. The obtained effective thermal conductivity distributions follow the normal distribution like the temperatures shown in Fig. 10. As shown in Fig. 12 (e), the change of mean effective thermal conductivities between different pellet size are less than 1%. Thus, it can be concluded that mean value (μ) of effective thermal conductivities are insensitive to the pellet size. However, as shown in Fig. 12 (f), standard deviation does show a little sensitivity to the pellet size comparing to the mean value, which might be caused by the limited number of data points used for this study since only 60 simulated were performed for each case.

6. Implications

By showing the calculated mean effective thermal conductivity values with and without heat generation in Fig. 13, this study necessitates the consideration of heat generation in individual fuel particles for the evaluation of the peak pellet temperature. The thermal conductivity models developed for the reference FCM and cermet fuel provide different mean effective thermal conductivity values and their statistical uncertainties due to random packing. The developed methodology and models provide a practical methodology to predict statistically-informed peak and average fuel temperatures of nuclear fuel pellets of heat generating particles. The statistical distribution of the effective thermal conductivities presented in this study is useful to estimate the uncertainty and confidence of the nuclear fuel temperature. Yet, the uncertainties of effective thermal conductivity shown as the standard deviation due to the random arrangements may not be significant compared to uncertainties in the experimental measurements of material properties and irradiation effects.

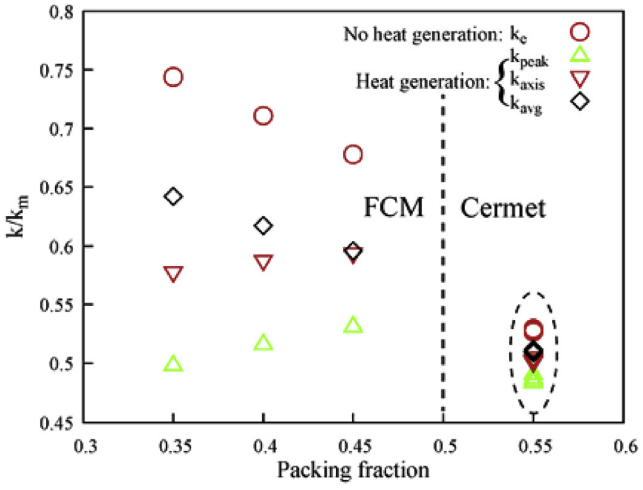

Fig. 13. Comparison of the calculated mean effective thermal conductivities of the FCM/cermet fuel pellet with and without individual fuel particle heat generation in the fuel kernel.

7. Conclusion

A key design and safety challenge for particle-based nuclear fuel is uniquely rooted in the random packing of excessive numbers of fuel particles. That is, the randomness of their locations call for a statistical treatment for fuel behavior. In reality, each particle is subject to different thermal boundary conditions, as its position with respect to neighboring particles is different due to random packing.

In this study, an enabling methodology for the evaluation of effective thermal conductivity of pellets with randomly distributed heat generating TRISO particles was developed using an in-house developed code and ANSYS 18. By combining the two codes, it was possible to generate three-dimensional FEM heat conduction models of multiple heat–generating fuel particles with multi-layers randomly dispersed in a matrix. Effective thermal conductivities were calculated using the peak particle temperature (k_{peak}), pellet centerline average temperature (k_{axis}), and pellet average temperature (k_{avg}) of the simulated FCM and cermet fuel pellets. Parametric sensitivity analysis with respect to packing fraction and pellet size was conducted to explore how effective thermal conductivity is affected by the random arrangement of fuel particles.

This study demonstrates the impact of randomly distributed heat source on the peak and average temperature of the TRISO fuel pellet. In light of this, three models that capture the particle heat generation effect are developed for the prediction of the peak particle temperature, fuel pellet centerline average temperature and fuel pellet average temperature of the reference FCM and cermet pellets using conventional heat conduction equation. The statistical distribution of the effective thermal conductivity due to random heat source arrangements exhibits the normal distribution whose spread is sensitively dependent on packing fraction. Higher packing fraction led to a narrower statistical spread of effective thermal conductivities by reducing the degree of freedom in the particle arrangements. It is important to point out that (1) the models presented in the present study is rather a supplement of existing models for the estimation of the peak particle temperature, and (2) the uncertainties of effective thermal conductivity due to the random arrangements may not be significant compared to uncertainties in the experimental measurements of material properties and irradiation effects.

Acknowledgements

This work was supported by Los Alamos National Laboratory Subcontract Award, Designing of Fuel Performance Experiments to be Performed Using the Annular Core Research Reactor (ACRR) (#397838).

Nomenclature

k	thermal conductivity, W/(m·K)

k_{peak}	thermal conductivity defined using fuel pellet peak particle temperature, W/(m·K)
k_{axis}	thermal conductivity defined using fuel pellet average axial temperature, W/(m·K)
k_{avg}	thermal conductivity defined using fuel pellet average temperature, W/(m·K)
L_p	FCM fuel pellet height, m
q'	linear power, W/m
q''	heat flux, W/m^2
q'''	power density, W/m^3
r_1	outer radius of the fuel kernel, m
r_2	outer radius of the buffer layer, m
r_3	outer radius of the OPyC layer, m
r_4	outer radius of the SiC layer, m
r_5	outer radius of the OPyC layer, m
R_p	fuel pellet radius, m
T	temperature, °C
T_R	surface temperature, °C

Greek symbols

β	variable defined in eq. (6)
ϕ	packing fraction
κ	variable defined in eq. (6)

Subscripts

p	particle
max	maximum value
TRISO	TRISO particle
1	fuel kernel of the TRISO particle
2	Buffer layer of the TRISO particle
3	IPyC layer of the TRISO particle
4	SiC layer of the TRISO particle
5	OPyC layer of the TRISO particle

References

[1] D.A. Petti, J. Buongiorno, J.T. Maki, R.R. Hobbins, G.K. Miller, Key differences in the fabrication, irradiation and high temperature accident testing of US and German TRISO-coated particle fuel, and their implications on fuel performance, Nucl. Eng. Des. 222 (2) (2003) 281–297.

[2] J.J. Powers, B.D. Wirth, A review of TRISO fuel performance models, J. Nucl. Mater. 405 (1) (2010) 74–82.

[3] P. Mills, R. Soto, G. Gibbs, Next Generation Nuclear Plant Pre-conceptual Design Report, Idaho National Laboratory (INL), 2007. INL/EXT-07-12967.

[4] J. Hughes, M. Liu, B. Wallace, A. Ali, M.R. Denman, N. Zweibaum, P. Peterson, E.D. Blandford, On the Question of Decay Heat Removal System Redundancy for Fluoride Salt-cooled High-temperature Reactors (FHR), ICAPP 2016, San Francisco, CA, USA, 2016, pp. 1973–1985.

[5] D. Hartanto, Y. Kim, F. Venneri, Neutronics evaluation of a super-deep-burn with TRU fully ceramic microencapsulated (FCM) fuel in CANDU, Prog. Nucl. Energy 83 (2015) 261–269.

[6] Y. Lee, B. Cho, N.Z. Cho, Steady-and transient-state analyses of fully ceramic microencapsulated fuel with randomly dispersed tristructural isotropic particles via two-temperature homogenized Model—I: theory and method, Nucl. Eng. Technol. 48 (3) (2016) 650–659.

[7] M.E. Stewart, A Historical Review of Cermet Fuel Development and the Engine Performance Implications, Nuclear and Emerging Technologies for Space 2015, Albuquerque, New Mexico, US, 2015.

[8] J.J. Powers, W.J. Lee, F. Venneri, L.L. Snead, C. Jo, D. Hwang, J. Chun, Y. Kim, K.A. Terrani, Fully Ceramic Microencapsulated (FCM) Replacement Fuel for LWRs, Oak Ridge National Laboratory and Korea Atomic Energy Research Institute, 2013. ORNL/TM-2013173, KAERI/TR-5136/2013.

[9] K.A. Terrani, L.L. Snead, J.C. Gehin, Microencapsulated fuel technology for commercial light water and advanced reactor application, J. Nucl. Mater. 427 (1) (2012) 209–224.

[10] B.P. Collin, Modeling and analysis of UN TRISO fuel for LWR application using the PARFUME code, J. Nucl. Mater. 451 (1) (2014) 65–77.

[11] N.R. Brown, H. Ludewig, A. Aronson, G. Raitses, M. Todosow, Neutronic evaluation of a PWR with fully ceramic microencapsulated fuel. Part I: lattice benchmarking, cycle length, and reactivity coefficients, Ann. Nucl. Energy 62 (2013) 538–547.

[12] A. Craft, R. O'brien, S. Howe, J. King, Submersion criticality safety of tungsten-rhenium urania cermet fuel for space propulsion and power applications, Nucl. Eng. Des. 273 (2014) 143–149.

[13] J.V. Miller, Estimating thermal Conductivity of Cermet Fuel Materials for Nuclear Reactor Application, 1967. NASA TN D-3898.

[14] J. Rosales, J. Perez, C. Garcia, A. Munnoz, C. Lira, Comparative study of random and uniform models for the distribution of TRISO particles in HTR-10 fuel elements, in: Proceedings of XV Workshop on Nuclear Physics IX International Symposium on Nuclear and Related Techniques, Havana, Cuba, 2015.

[15] J. Wang, J.K. Carson, M.F. North, D.J. Cleland, A new approach to modelling the effective thermal conductivity of heterogeneous materials, Int. J. Heat Mass Tran. 49 (17) (2006) 3075–3083.

[16] A. Pereira, C. Matt, M. Cruz, Numerical prediction of the effective thermal conductivity of fibrous composite materials, in: 9th AIAA/ASME Joint Thermophysics and Heat Transfer Conference, 2006, p. 3429.

[17] K. Pietrak, T.S. Wisniewski, A review of models for effective thermal conductivity of composite materials, J. Power Technol. 95 (1) (2015) 14.

[18] J.C. Maxwell, A Treatise on Electricity and Magnetism, Clarendon press, 1881.

[19] R. Hamilton, O. Crosser, Thermal conductivity of heterogeneous two-component systems, Ind. Eng. Chem. Fund. 1 (3) (1962) 187–191.

[20] D. Hasselman, L.F. Johnson, Effective thermal conductivity of composites with interfacial thermal barrier resistance, J. Compos. Mater. 21 (6) (1987) 508–515.

[21] D. Jeffrey, Group expansions for the bulk properties of a statistically homogeneous, random suspension, in: Proceedings of the Royal Society of London a: Mathematical, Physical and Engineering Sciences, The Royal Society, 1974, pp. 503–516.

[22] D.J. Jeffrey, Conduction through a random suspension of spheres, in: Proceedings of the Royal Society of London a: Mathematical, Physical and Engineering Sciences, The Royal Society, 1973, pp. 355–367.

[23] Y. Chiew, E. Glandt, The effect of structure on the conductivity of a dispersion, J. Colloid Interface Sci. 94 (1) (1983) 90–104.

[24] E.E. Gonzo, Estimating correlations for the effective thermal conductivity of granular materials, Chem. Eng. J. 90 (3) (2002) 299–302.

[25] C. Folsom, C. Xing, C. Jensen, H. Ban, D.W. Marshall, Experimental measurement and numerical modeling of the effective thermal conductivity of TRISO fuel compacts, J. Nucl. Mater. 458 (2015) 198–205.

[26] Y. Agari, A. Ueda, S. Nagai, Thermal conductivities of composites in several types of dispersion systems, J. Appl. Polym. Sci. 42 (6) (1991) 1665–1669.

[27] V.D. Bruggeman, Berechnung verschiedener physikalischer Konstanten von heterogenen Substanzen. I. Dielektrizitätskonstanten und Leitfähigkeiten der Mischkörper aus isotropen substanzen, Ann. Phys. 416 (7) (1935) 636–664.

[28] L. Grossman, Thermal conductivity of coated particle UO_2-tungsten cermets, NASA (1968). NASA CR-1154.

[29] W.M. Rohsenow, J.P. Hartnett, Y.I. Cho, Handbook of Heat Transfer, McGraw-Hill, New York, 1998.

[30] I. Nozad, R. Carbonell, S. Whitaker, Heat conduction in multiphase systems—I: theory and experiment for two-phase systems, Chem. Eng. Sci. 40 (5) (1985) 843–855.

[31] M.E. Cruz, A.T. Patera, A parallel Monte-Carlo finite-element procedure for the analysis of multicomponent random media, Int. J. Numer. Meth. Eng. 38 (7) (1995) 1087–1121.

[32] R.P. Rocha, M.A.E. Cruz, Computation of the effective conductivity of unidirectional fibrous composites with an interfacial thermal resistance, Numer. Heat Tran. Part a: Applications 39 (2) (2001) 179–203.

[33] C. Tien, K. Vafai, Statistical bounds for the effective thermal conductivity of microsphere and fibrous insulation, in: 2nd Thermophysics and Heat Transfer Conference, 1978.

[34] T. Oppelt, T. Urbaneck, H. Böhme, B. Platzer, Numerical investigation of effective thermal conductivity for two-phase composites using a discrete model, Appl. Therm. Eng. 115 (2017) 1–8.

[35] T.W. Cho, D.-S. Sohn, Y.S. Kim, Thermal conductivity of U–Mo/Al dispersion fuel: effects of particle shape and size, stereography, and heat generation: special Issue for ANFC2014, J. Nucl. Sci. Technol. 52 (10) (2015) 1328–1337.

[36] K. Bari, S.Z. Khan, T. Lowe, J.K. Farooqi, Measurement of thermal diffusivity for alumina borosilicate glass bearing TRISO fuel particles: experiment and modelling correlation, J. Mater. Sci. 48 (14) (2013) 4866–4875.

[37] J.A. Webb, I. Charit, Analytical determination of thermal conductivity of W–UO 2 and W–UN CERMET nuclear fuels, J. Nucl. Mater. 427 (1) (2012) 87–94.

[38] R. Stainsby, A. Grief, M. Worsley, F. Dawson, Investigation of Local Heat Transfer Phenomena in a Pebble Bed HTGR Core, AMEC NSS Limited, London, United Kingdom, 2009. NR001/RP/002 R01.